Journal of Rehabilitation in Civil Engineering 8-4 (2020) 15-27

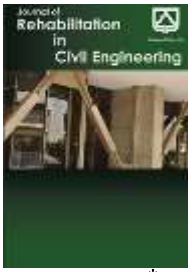

journal homepage: http://civiljournal.semnan.ac.ir/

Compressive Strength Assessment of Concrete Containing Metakaolin Using ANN

Y. Sharifi* and M. Hosseinpour
Department of Civil Engineering, Vali-e-Asr University of Rafsanjan, Rafsanjan, Iran

Corresponding author: *y.sharifi@vru.ac.ir*

ARTICLE INFO

Article history:
Received: 20 March 2019
Accepted: 24 June 2020

Keywords:
Artificial neural network,
Compressive strength of concrete,
Metakaolin,
Garson's algorithm,
Nonlinear least squares regression.

ABSTRACT

Artificial neural networks (ANNs) as a powerful approach have been widely utilized to demonstrate some of the engineering problems. A three-layer ANN including three neurons in the hidden layer is considered to produce a verified pattern for assessing the compressive strength of concrete incorporating metakaolin (MK). For this purpose, an extensive database including 469 experimental specimens was obtained from the literature. Next, novel equations utilizing the developed ANN approach were developed to measure the compressive strength of concrete mixtures incorporating MK. To examine the model accuracy a comparison between the proposed formulas based ANN and an empirical formula based nonlinear least-squares regression (NLSR) was carried out. The results show that the proposed formula based on the ANN yields a higher correlation coefficient and fewer errors compared to the NLSR method. An analysis based weights incorporating was utilized to show the significance of input variables. Accordingly, the ratio of fine aggregate to coarse aggregate exerts a dominant influence on the compressive strength of the concretes containing MK.

1. Introduction

Using pozzolana and mineral admixture as a replacement substance in concrete and mortar shows a significant modification in their properties. Recently, the addition of MK as an alternative pozzolana is considered more attention. MK obtained from calcining kaolin as a thermal procedure in the 700-850 ºC temperature range. Two important reasons for using MK are material durability and accessibility. Moreover, using filler and accelerated cement hydration together causes an early increase of strength in mortar and concrete. Besides, the shrinkage of concrete containing MK as cement replacement (up to 15%) is less than concrete without MK [1-22].

To date, many studies have been accomplished which pointed to the increase of compressive strength (f_c) in the concrete or mortar with MK, specifically at the initial

DOI: 10.22075/JRCE.2020.19043.1358

curing time. Wild et al. [10] examined the influence of MK in improving concrete strength. They used the range of 0-30% of MK for concretes by a curing period of 1 to 90 days. The obtained conclusions demonstrated that the optimum content of MK as cement replacement was about 20% to achieve maximum long term strength, also they found that strength improvement of concrete does not continue beyond 14 days regardless of the replacement ratio. Two groups of specimens with 36 mixes were made by Vu et al. [11]. In the first group by 6 samples the ratio of binder to sand measured 1:2.75, while in the second group by 30 specimens, the ratio of binder to sand was 1:2. Five values of MK were considered for these mixes including 10, 15, 20, 25, and 30 percent of MK replacing by cement weight, and also one mix without MK was considered as the control mix. They found that the compressive strength of mortars incorporating 10%, 15%, and 20% MK increased at 7, 28, 60, and 90 days. Also, for the mixes by 30% MK replacing by cement, the compressive strength of mortars decreased at 7, 28, 60, and 90 days. Another researcher, Parande et al. [12] replaced MK by cement weight in mortar specimens at the ratios of 5%, 10%, 15%, and 20%. These specimens had the water-cement ratio of 0.40 and binder-sand ratio of 1:3. They found that the compressive strength of the mortars with MK was increased until the end of 90 days. Also, it was found that the best outcomes were related to the specimens with 15% MK. In recent decades, the use of artificial intelligence in the different fields of civil engineering has grown widely [23-47]. In the current study, an ANN as a reliable and trustworthy branch of machine learning was carried out to assess the concrete compressive strength incorporating MK. In the published current papers, ANN has been used widely for different applications in engineering. The ANN is employed for input-output models. In the ANN models, experimental or numerical datasets are used for training the system. If the dataset obtains appropriate data on the problem, therefore the ANN training model contains sufficient data to produce the outputs and the model can be present as a reliable model. The performance of neural networks is described in detail in Section 3.

2. Experimental Dataset

In this article, the experimental dataset for use in the ANN model was obtained from 13 reliable technical kinds of literature [10-22]. The concrete strength incorporated with MK may be related to specimen age (AS), MK-binder ratio (MB), super plasticizer-binder ratio (SB), water-binder ratio (WB), binder-aggregate ratio (BA) and also fine aggregate-coarse aggregate ratio (FC). The statistics of these parameters as the ANN model inputs and output are tabulated in Table 1. Moreover, to illustrate the frequency of these parameters, the frequency histograms are shown in Fig. 1. It is clear from Fig.1 that the utilized database gives an efficient scattering to develop an accurate model.

3. ANN Approach

ANN was utilized to develop a new formula for the compressive strength in the concretes containing MK. As a result, the relationship between the influencing variables on the compressive strength in the concretes containing MK was attained through suitable ANN training. The most reputable class of ANN has been introduced as a multilayer perceptron (MLP). The MLP applies a feed-forward procedure for a generation. The MLP has been proposed as one of the robust networks for examination each continuous function in each desired accuracy. The feed-forward process examines one or several variable/s as output/s using foreteller inputs variables. The network process of feed-forward is based on the formation of the layer and connected synapses [48, 49]. Besides, a supervised algorithm that is used for multilayers networks was employed. The back-propagation (BP) process compares the obtained output from the algorithm to real value and adapts the results until the specified error obtained. The ANN generates using a trial and error process that each input variable defined by weight. Then the input of each node can be described by the following equation:

$$net_j = \sum_{i=1}^{n} w_{ij} x_i + b_j \qquad (1)$$

where net_j introduced as the node inputs; x_i, b_j, and w_{ij} are justified as the input, the bias, and the related weight values, respectively. Finally, the output is evaluated using the function generated for the present ANN.

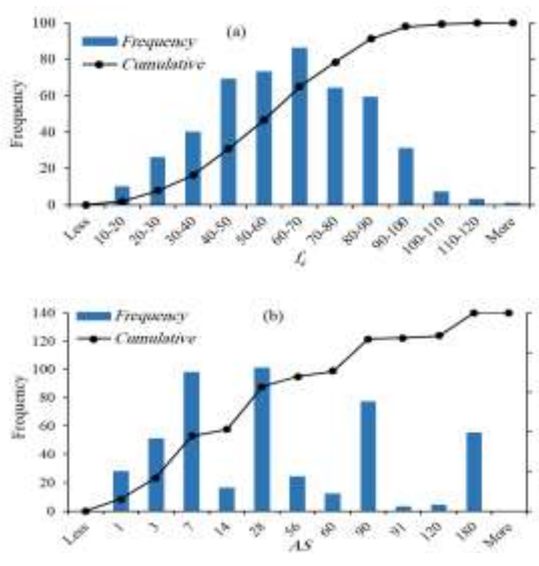

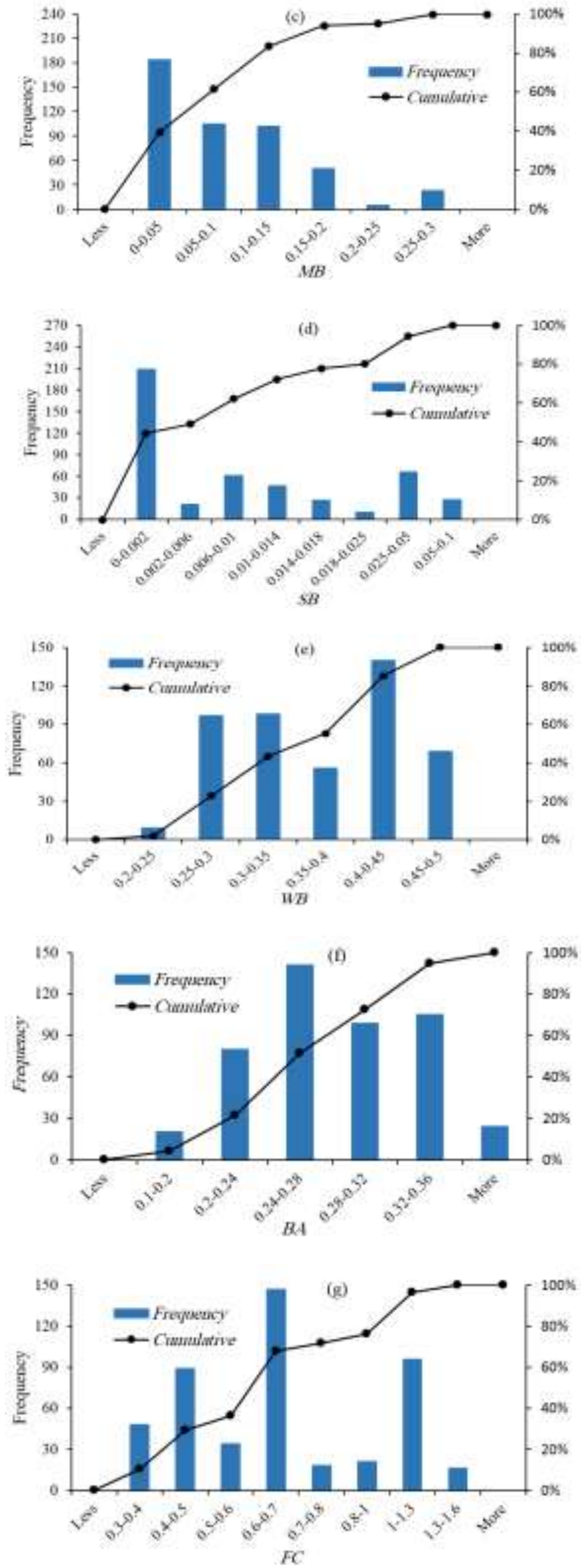

Fig. 1. Histograms graphs of the used variables used in the model construction.

Table 1. Statistics of the used parameters.

Parameter	f_c	*AS*	*MB*	*SB*	*WB*	*BA*	*FC*
Mean	61.7123	50.2473	0.0988	0.0144	0.3868	0.2424	0.7439
Std. Error of Mean	0.9697	2.6230	0.00374	0.0010	0.0035	0.0026	0.0143
Median	62.5000	28.0000	0.1000	0.0090	0.4000	0.2400	0.6600
Mode	67.00	28.00	0.00	0.00	0.45	0.29	1.22
Std. Deviation	21.0009	56.8039	0.0809	0.0224	.0765	0.0559	0.3105
Variance	441.038	3226.682	0.007	0.001	0.006	0.003	0.096
Skewness	-0.025	1.265	0.599	2.303	-0.001	-0.495	0.812
Std. Error of Skewness	0.113	0.113	0.113	0.113	0.113	0.113	0.113
Range	110.00	179.00	0.30	0.09	0.25	0.25	1.14
Minimum	10.30	1.00	0.00	0.00	0.25	0.10	0.31
Maximum	120.30	180.00	0.30	0.09	0.50	0.35	1.45

There are several transfer functions based ANN approach. Here, the outputs function was identified as below:

$$out_j = f\left(net_j\right) \tag{2}$$

where out_j and f identify as the output and transfer function, respectively. Fig. 2 shows the neural network procedure.

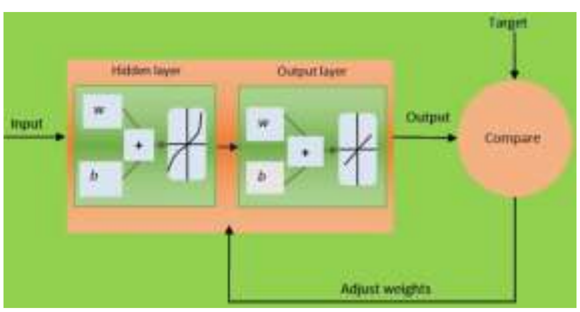

Fig. 2. Arrangement of a simple ANN.

3.1. ANN Training

In the present research the Levenberg-Marquardt (LM) algorithm was utilized [49]. Each epoch presents one forward and one backward pass of all training samples. The LM algorithm is an amendment of the Back-Propagation (BP) procedure [50], therefore:

By supposing the $W(\underline{x})$ as a function, it can be minimized as below:

$$\Delta\underline{x} = -\left[\nabla^2 W(\underline{x})\right]^{-1} \nabla W(\underline{x}), \tag{3}$$

where $\nabla^2 W(\underline{x})$ and $\nabla W(\underline{x})$ identified as the Hessian matrix and the gradient, respectively. $W(\underline{x})$ can be presented as:

$$W(\underline{x}) = \sum_{i=1}^{N} e_i^2(\underline{x}), \tag{4}$$

and,

$$\nabla W(\underline{x}) = J^T(\underline{x})\, \underline{e}(\underline{x}) \tag{5}$$

$$\nabla^2 W(\underline{x}) = J^T(\underline{x})\, J(\underline{x}) + S(\underline{x}) \tag{6}$$

where $J(\underline{x})$ recognized as the Jacobian matrix. S(x) can be identified as below:

$$S(\underline{x}) = \sum_{i=1}^{N} e_i(\underline{x})\ \nabla^2 e_i(\underline{x}) \tag{7}$$

By utilizing the Gauss-Newton procedure, $S(\underline{x}) = 0$ the Eq. (3) considered as:

$$\Delta\underline{x} = \left[J^T(\underline{x})\ J(\underline{x})\right]^{-1} J^T(\underline{x})\ \underline{e}(\underline{x}) \tag{8}$$

The LM development can be presented as:

$$\Delta\underline{x} = [J^T(\underline{x})\, J(\underline{x}) + \mu I]^{-1} J^T(\underline{x})\ \underline{e}(\underline{x}) \tag{9}$$

In each step depends on the increasing or decreasing the $w(\underline{x})$, a parameter multiplied or divided.

3.2. Efficiency Criterions

Three criteria are employed for demonstrate the efficiency of the obtained equations. The following parameters introduced as the mean absolute error (*MAE*), mean squared error (*MSE*), and correlation coefficient (*R*). The above-mentioned parameters can be evaluated as:

$$MAE = \frac{1}{N}\sum_{i=1}^{N}|y_i - t_i| \tag{10}$$

$$MSE = \frac{1}{N}\sum_{i=1}^{N}(t_i - y_i)^2 \tag{11}$$

$$R = \frac{\sum_{i=1}^{N}(y_i - \bar{y}_i)(t_i - \bar{t}_i)}{\sqrt{\sum_{i=1}^{N}(y_i - \bar{y}_i)^2 \sum_{i=1}^{N}(t_i - \bar{t}_i)^2}} \tag{12}$$

where N indicates the specimens numbers, t_i and $\bar{t}_i$ indicate the exact and the mean of the outputs, respectively, and y_i and $\bar{y}_i$ indicate the examined and the mean of the examined outputs, respectively (for the ith output).

3.3. ANN Development to f_c Prediction of Concretes Containing MK

The experimental dataset was used for establishing the ANN-based model for representing the compressive capacity of the concretes incorporating MK. The recognition of the parameters which affect the *fc* of concretes containing MK is difficult and, the effective parameters are not independent of each other and some of them may be strongly related together. But normally age of specimen (*AS*), MK-binder ratio (*MB*), super plasticizer-binder ratio (*SB)*, water-binder ratio (*WB*), binder-aggregate ratio (*BA*) and fine aggregate to the coarse aggregate ratio (*FC*) are considered as the parameters which can affect on the *f*c of the concretes containing MK. Therefore, in this study, the initial input and output parameters was chosen as follows:

$$Input = \{AS, MB, SB, WB, BA, FC\}$$
$$Output = \{f_c\}$$

The number of nodes affects the efficiency of the BP network, the ideal hidden nodes number is specified by the trial-and-error process. Therefore, to achieve an appropriate network, ten networks were constructed. These networks contained 1-10 nodes in the hidden layer, respectively. Fig. 3 and 4 show MSE and R values for all constructed networks by a different number of hidden layer neurons, respectively. As can be seen from these figures, by enhancement of hidden layer neuron numbers, the network gives a more exact output. On the other hand, each network containing more hidden layer neurons results a tedious and lengthy equation. Therefore, by considering the accuracy of the model, in the current paper, a model by three hidden layer nodes is considered.

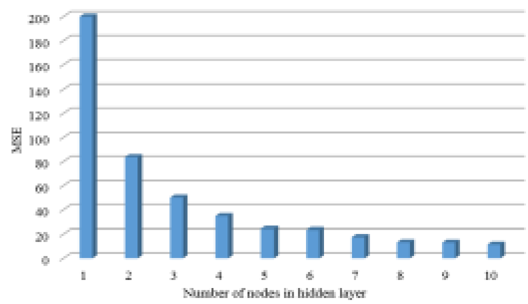

Fig. 3. The MSE of the several networks using different hidden layer nodes.

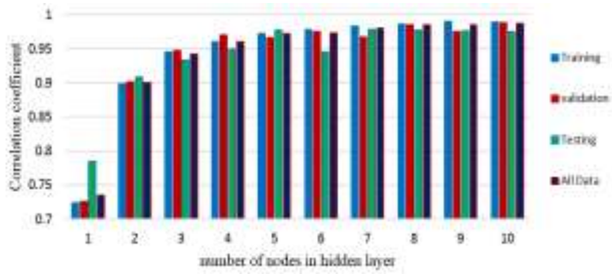

Fig. 4. The correlation coefficient for different networks.

Over-fitting is one of the problems that may be happened during the training generation. The mentioned coincidence leads to the network gives a small quantity error in the training phase, but by providing more samples to the system the error quantity arises. To dominate the event aforementioned above an early stopping procedure was utilized to pass the over-fitting. As mentioned, the database was distributed in three groups concluding, training, validating, and testing. While the error in validating set increases, the training state is regenerated, and the weights invalidating rule are returned. In other words, the validating set is utilized to avoid the over-fitting process, which causes network estimates suitable estimations of the different samples (Fig.5).

In this article, the data distributed into three sets from a random selection, 70% was utilized at the training set, 15% was utilized at the validation set, and 15% was utilized at the testing set. Accordingly, from 469 data 329 specimens were introduced as the training set, for validation and testing sets 70 specimens were introduced.

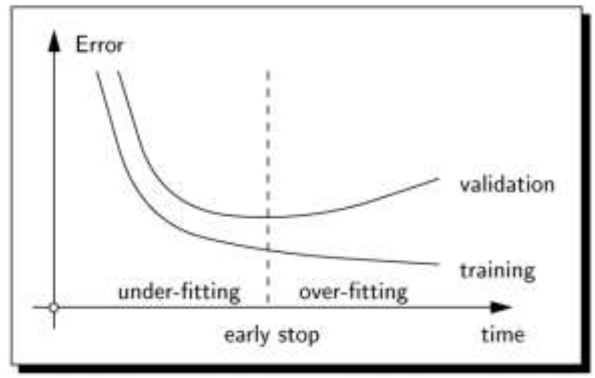

Fig. 5. The over-fitting coincidence [51].

The used data in the training set give an important issue and it is mainly related to the reliability of the model [52]. Frank and Todeschini [53] discuss that the minimum ratio of the dataset numbers to the input numbers to generate a powerful network is three. Moreover, they recommended a ratio of five to obtain a more reasonable model. Here, the mentioned ratio calculated as 469/6=78.2. The input and output variables standardized as follows:

$$X_{si} = \frac{X_i - Mean}{SD} \tag{13}$$

where Xi is variable values, Mean and SD present the mean and standard deviation of variables, respectively.

The applied variables for the model were six parameters and fc of concrete was the output. The input and output layers comprised of six and one neurons, respectively. Consequently, an ANN modeling concluding three hidden layer neurons modified as LM/BP learning algorithm was established. The Log-Sigmoid was utilized as a transfer function to derive the formulae in explicit form. The predicted results of fc obtained using the ANN model are illustrated in Fig. 6. It is shown in Fig. 6

that training, validation, and testing data sets yield enough strong relation between experimental and obtained results.

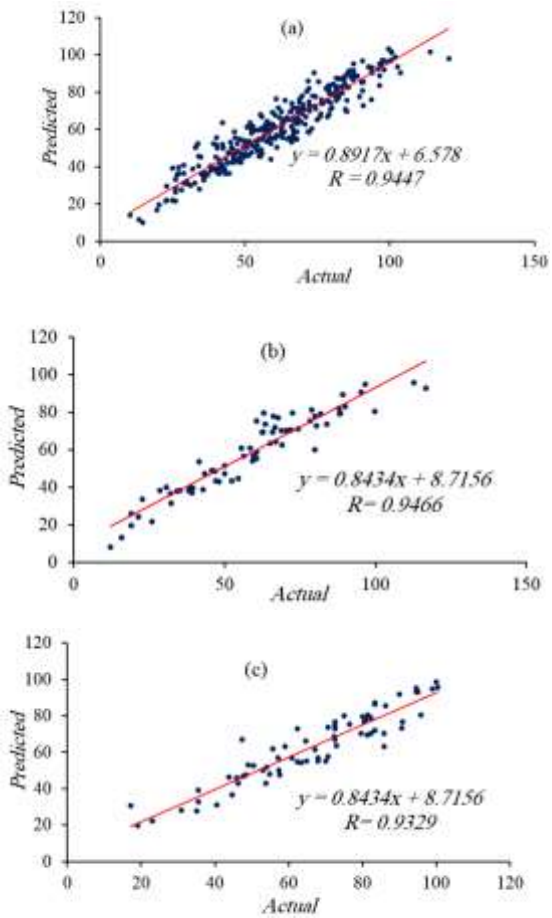

Fig. 6. The correlation values between experimental and obtained quantities using the ANN model in (a) Training set, (b) validation set, and (c) testing set.

3.4. ANN-Based Model

The closed-form equation can be established using the constructed ANN model to evaluate the f_c of concretes. The output of each network can be stated as follow:

$$\text{output} = f\left(W_2 \times \left(f\left(W_1 \times X + b_1\right)\right) + b_2\right) \qquad (14)$$

where W_1 and W_2 introduced as the first and second layers weight matrix, respectively, moreover b_1 and b_2 show the first and second layer bias vector. Then, the aforementioned matrix may be represented as below:

$$\text{output} = f\left(W_2 \times \begin{bmatrix} 1 \\ f\left(W_1 \times X\right) \end{bmatrix}\right),$$

$$X = \begin{bmatrix} 1 & x_1 & x_2 & x_3 & x_4 & x_5 & x_6 \end{bmatrix}^T$$

$$W_1 = \begin{bmatrix} b_{A1} & W_{1,A1} & W_{2,A1} & W_{3,A1} & W_{4,A1} & W_{5,A1} & W_{6,A1} \end{bmatrix}$$

$$W_2 = \begin{bmatrix} b_{out} & W_{A1,out} \end{bmatrix}$$

Finally, the equation using the ANN model for measuring the f_c is presented as follows:

$$f_c = -\frac{60.903}{1+e^{-\beta_1}} + \frac{481.780}{1+e^{-\beta_2}} - \frac{285.565}{1+e^{-\beta_3}} - 206.815 \qquad (15)$$

Table 2. The formulae efficiency for f_c predictions.

Method	Training			Validation			Testing		
	R	MSE	MAE	R	MSE	MAE	R	MSE	MAE
Proposed equation ANN	0.9447	44.9074	5.0847	0.9466	59.0875	5.7493	0.9329	65.2862	6.1648
Proposed equation NLSR	0.8404	122.9463	8.7153	0.8582	171.2325	10.1029	0.8427	122.0167	9.0370

$$\beta_1 = 0.005(AS) - 0.8024(MB) + 16.6971(SB) + 7.5586(WB) + 28.6450(BA) + 21.9965(FC) - 28.2746$$

$$\beta_2 = 0.2456(AS) - 1.6123(MB) - 3.0228(SB) + 0.6516(WB) + 0.5805(BA) - 0.6097(FC) - 2.2880$$

$$\beta_3 = -0.0014(AS) - 0.5714(MB) - 0.1884(SB) + 2.6995(WB) - 0.4965(BA) - 1.0784(FC) + 0.6751$$

4. NLSR Based Model

One of the conventional methods applied in classic modeling is regression analysis. The nonlinear least-squares regression (NLSR) was applied in this article as a classical method to compare with the ANN model. As a result, several formulations based on the NLSR were developed using the SPSS program to predict the fc of concrete. According to the maximum R-value, the best formulation is chosen as follow:

$$f_c = \exp\begin{pmatrix} 2.024AS^{0.057} + 0.186MB - 0.234SB \\ + 0.671WB^{-0.732} + 0.006BA^{-1.391} \\ + 0.201FC^{-0.269} \end{pmatrix} \quad (16)$$

5. Models Verification

Performance statistics of the proposed formulations using the ANN and NLSR methods are presented in Table 2. The parameters of R, MSE, and MAE are chosen to assess the performance of the presented formulation. For model validity, accepted criteria introduced by Gandomi *et al.* [54] which suggested by Smith [55]. This criteria expressed as follows:

1- There is a powerful relation if |R| > 0.8.

2- There is a suitable relation if 0.2 < |R| < 0.8.

3- There is a weak relation if |R| < 0.2.

Moreover, it is clear that for a strong model, the error values have to be at a minimum. The evaluation measures presented in Table 2 confirm that the proposed formulations (Eq. 16 and Eq. 17) are capable for prediction of f_c in the concretes containing MK; however, the proposed equation using the ANN method demonstrated more degree of accuracy than classic modeling based on the nonlinear regression analysis. Furthermore, for more comparison, the obtained results and experimental data have been plotted as shown in Fig. 7. It is clear that as the ratios of experimental to predicted value are close to one, the model yields proper accuracy. Therefore, according to Fig. 7, the distribution of the actual to evaluated ratios shows remarkable accuracy of the proposed ANN formulation. Moreover, it is obvious from Fig. 7 that the ANN formulae have more precision than NLSR formulae as a classical model.

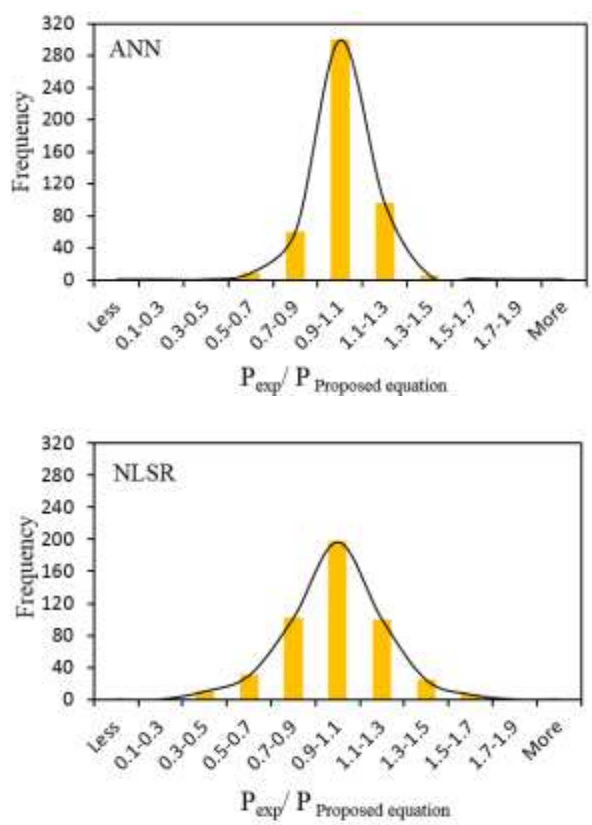

Fig. 7. A comparison of ANN and NLSR of experimental to proposed equation ratio of concrete.

6. Importance Analysis

A sensitivity analysis was assessed to specify the importance of all input variables. Garson's algorithm [56] is used to compute the comparative value of the input variables. Fig. 8 illustrates the procedure of this algorithm. An example to show the Garson's algorithm is clarified as below:

1- The contribution of inputs through input-hidden-output linkage evaluates (e.g., $C_{Aa}=W_{Aa}\times W_{oA}$).

2- The inputs relative contributions evaluates (e.g., $r_{Aa}=|C_{Aa}|/|C_{Aa}+C_{Ab}+C_{Ac}|$).

3- The input relative contributions are summed (e.g., $S_a=r_{Aa}+r_{Ba}$).

4- The relative importance of each input (r_I) evaluates (e.g., $r_{Ia}=S_a/(S_a+S_b+S_c)$).

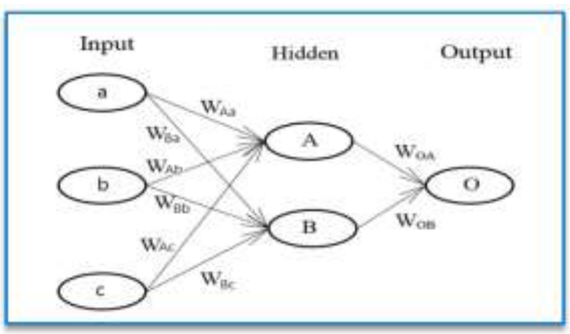

Fig. 8. The ANN structure used in Garson's algorithm.

Fig. 9 shows the significance of input parameters, as it is clear in this figure the ratio of fine aggregate to coarse aggregate (*FC*) and the age of specimen (*AS*) exert dominant effects on the f_c, respectively. Also, according to this figure, the ratio of superplasticizer to binder (*SB*) exerts minimum influences on the *fc* of this type of concrete.

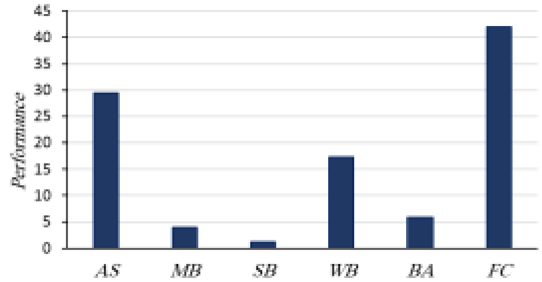

Fig. 9. Variable significance in the developed ANN model.

Moreover, to show the accuracy of the developed ANN, an alternative analysis was accomplished using the method proposed in [57, 58]. The mentioned procedure examines the reaction of the produced equation to a set of assumed data. Based on this method, one input is changed while the other inputs remain constant at their average. If this analysis yields confirmed results to the underlying problem, the strength of developed formulae is proved. For this study, the results of the mentioned parametric analysis show in Fig. 10.

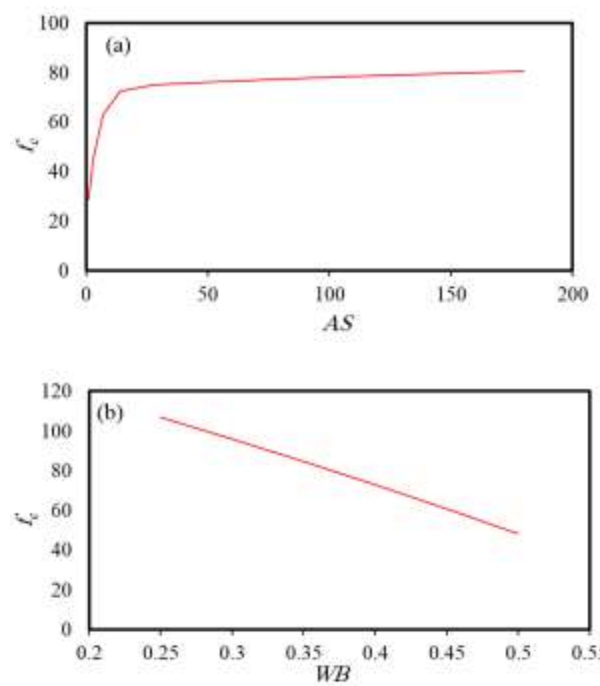

Fig. 10. Parametric analysis of compressive strength for concretes containing MK in the ANN model.

The tendency of the f_c to the variations of the two parameters including *AS* and *WB* is shown in Fig.10. As we expected, the *fc* of concrete increases by increasing of *AS* and also *fc* of concrete decreases by increasing of *WB* ratio from 0.25 to 0.5. Therefore, these results confirm that the proposed formula based ANN gives exact results for practical engineering applications.

7. Conclusions

In the current study, the ANN was applied to assess the f_c. The experimental dataset including 469 specimens was obtained using 13 reliable technical kinds of literature for ANN model development. Consequently, the ANN model including three hidden layer neurons was constructed and six input parameters were considered including the age of the specimen, MK-binder, super plasticizer-binder, water-binder, binder-aggregate, and fine aggregate-coarse aggregate ratios. At the next, the new formulae based on ANN were presented and performance analysis was undertaken for confirmation of this formulae. Also, a comparison was made between the ANN model and the nonlinear least squares regression model as a classical method. it can be concluded that the ANN formulation based model gives more exactness than the NLSR model. In the end, the importance of input parameters was determined using Garson's algorithm and it was found that the ratio of fine aggregate to coarse aggregate exerts more influence on the f_c than other input parameters. As a final point, the most important of the present research was to generate a precise equation to assess the compressive strength of concretes containing MK. The new proposed formulae can be used by practical engineering applications.

REFERENCES

[1] Y Sharifi, I Afshoon, Z Firoozjaei, M Momeni (2016). Utilization of Waste Glass Micro-particles in Producing Self-Consolidating Concrete Mixtures. International Journal of Concrete Structures and Materials 10 (3): 337–353.

[2] Y Sharifi, I Afshoon, Z Firoozjaie (2015). Fresh properties of self-compacting concrete containing ground waste glass microparticles as cementing material. Journal of Advanced Concrete Technology 13 (2): 50-66.

[3] I Afshoon, Y Sharifi (2014). Ground copper slag as a supplementary cementing material and its influence on the fresh properties of self-consolidating concrete. The IES Journal Part A: Civil & Structural Engineering 7 (4): 229-242.

[4] Gleize, PJP. Cyr, M. Escadeillas, G. (2007). Effects of metakaolin on autogenous shrinkage of cement pastes. Cement Concrete Compos; 29(2):80-7.

[5] Sabir, B.B. Wild, S. Bai, J. (2001). Metakaolin and calcined clays as pozzolans for concrete: a review. Cement Concrete Compos; 23(6): 441-54.

[6] Heidari A, Hashempour M, Chermahini MD. (2019) Influence of reactive MgO hydration and cement content on C&DW aggregate concrete characteristics. International Journal of Civil Engineering. 1;17(7):1095-106.

[7] Shakiba M, Rahgozar P, Elahi AR, Rahgozar (2018) R. Effect of Activated Pozzolan with Ca (OH) 2 and nano-SiO2 on Microstructure and Hydration of High-Volume Natural Pozzolan Paste. Civ Eng J. 30; 4(10):2437-49.

[8] Sharifi YA, Maghsoudi AA, Rahgozar RE. (2010) Ductility of Self-Consolidating Reinforced Concrete Beams. Civil Engineering Infrastructures Journal. 1;44(4):497-506.

[9] Kakvand, P., Rahgozar, R., Ghalehnovi, M. and Irandegani, M.A. (2014) 'Experimentally analysing compressive and tensile strengths of concrete containing

steel waste fibers', Int. J. Structural Engineering, Vol. 5, No. 2, pp.132–141.

[10] Wild, S. Khatib, J.M. Jones, A. (1996). Relative strength, pozzolanic activity and cement hydration in superplasticised metakaolin concrete. Cement and Concrete Research, Vol. 26, No. 10, pp. 1537-1544.

[11] Vu, D.D. Stroeven, P. Bui, V.B. (2001). Strength and durability aspects of calcined kaolin-blended Portland cement mortar and concrete. Cement Concrete Compos; 23 (6):471-8.

[12] Parande, A.K. Babu, B.R. Karthik, M.A. (2008) Deepak Kumaar KK, Palaniswamy N. Study on strength and corrosion performance for steel embedded in metakaolin blended. concrete/mortar. Constr Build Mater; 22(3): 127-34.

[13] Li, Q. Geng, H. Shui, Zh. Huang, Y. (2015). Effect of metakaolin addition and seawater mixing on the properties and hydration of concrete. Applied Clay Science 115 - 51–60.

[14] Safarzadegan Gilan, S. Bahrami Jovein, H. Ramezanianpour, A. (2012). Hybrid support vector regression – Particle swarm optimization for prediction of compressive strength and RCPT of concretes containing metakaolin. Construction and Building Materials 34 -321–329.

[15] Wong, H.S, Abdul Razak, H. (2005). Efficiency of calcined kaolin and silica fume as cement replacement material for strength performance. Cement and Concrete Research 35 - 696– 702.

[16] Poon, C.S. Kou S.C. Lam, L. (2006). Compressive strength, chloride diffusivity and pore structure of high performance metakaolin and silica fume concrete. Construction and Building Materials 20-858–865.

[17] Ramezanianpour, A.A. Bahrami Jovein, H. (2012). Influence of metakaolin as supplementary cementing material on strength and durability of concretes. Construction and Building Materials 30-470–479.

[18] Guneyisi, E. Gesogˇlu, M. Karaogˇlu, S. Mermerdaş, K. (2012). Strength, permeability and shrinkage cracking of silica fume and metakaolin concretes. Construction and Building Materials 34-120–130.

[19] Mohammadi, M. Mir Moghtadaei, R. Ashraf Samani, N. (2014). Influence of silica fume and metakaolin with two different types of interfacial adhesives on the bond strength of repaired concrete. Construction and Building Materials 51-141–150.

[20] Khatib, J.M. (2008). Metakaolin concrete at a low water to binder ratio. Construction and Building Materials 22 -1691–1700.

[21] Duana, P. Shuia, Z.h. Chena, W. Shenb, C.h. (2013). Enhancing microstructure and durability of concrete from ground granulated blast furnace slag and metakaolin as cement replacement materials. J. Mater. Res. Technol; 2(1):52-59.

[22] Khatib, M.J. Hibbert, J.J. (2005). Selected engineering properties of concrete incorporating slag and metakaolin. Construction and Building Materials 19-460–472.

[23] Naderpour H, Eidgahee DR, Fakharian P, Rafiean AH, Kalantari SM. (2019). A new proposed approach for moment capacity estimation of ferrocement members using Group Method of Data Handling. Engineering Science and Technology, an International Journal. 23 (2), 382-391.

[24] Rezazadeh Eidgahee D, Haddad A, Naderpour H. (2018). Evaluation of shear strength parameters of granulated waste rubber using artificial neural networks and group method of data handling. Scientia Iranica.

[25] Naderpour H, Nagai K, Fakharian P, Haji M. (2019). Innovative models for prediction of compressive strength of FRP-confined circular reinforced concrete columns using soft computing methods. Composite Structures. 215: 69-84.

[26] Tohidi S. and Sharifi Y. (2015). Empirical modeling of distortional buckling strength of half-through bridge girders via stepwise regression method. Advances in Structural

Engineering, Vol. 18, No. 9, pp. 1383-1397.

[27] Hosseinpour M., Sharifi H. and Sharifi Y. (2018). Stepwise regression modeling for compressive strength assessment of mortar containing metakaolin. International Journal of Modelling and Simulation, Vol. 38, No. 4, pp. 207-215.

[28] Sharifi Y. and Moghbeli A. (2019). Stepwise Regression for shear capacity assessment of steel fiber reinforced concrete beams. Journal of Rehabilitation in Civil Engineering, Vol. 7, No. 2, pp. 95-108.

[29] Eidgahee DR, Rafiean AH, Haddad A. A (2019). Novel Formulation for the Compressive Strength of IBP-Based Geopolymer Stabilized Clayey Soils Using ANN and GMDH-NN Approaches. Iranian Journal of Science and Technology, Transactions of Civil Engineering.

[30] Sharifi, Y. Hosseinpour, M. (2019). Adaptive neuro-fuzzy inference system and stepwise regression for compressive strength assessment of concrete containing metakaolin. International Journal of Optimization in Civil Engineering; 9 (2):251-272.

[31] Naderpour H, Rafiean AH, Fakharian P. Compressive strength prediction of environmentally friendly concrete using artificial neural networks. Journal of Building Engineering 16: 213–219.

[32] Naderpour H, Nagai K, Haji M, Mirrashid M. Adaptive neuro-fuzzy inference modelling and sensitivity analysis for capacity estimation of fiber reinforced polymer-strengthened circular reinforced concrete columns. Expert Systems. 2019:e12410.

[33] Naderpour H, Kheyroddin A, Amiri GG. Prediction of FRP-confined compressive strength of concrete using artificial neural networks. Composite Structures. 2010 Nov 1;92(12):2817-29.

[34] Naderpour H, Alavi SA. A proposed model to estimate shear contribution of FRP in strengthened RC beams in terms of Adaptive Neuro-Fuzzy Inference System. Composite Structures. 2017 Jun 15;170:215-27.

[35] Sharifi Y., Lotfi F. and Moghbeli A. Compressive strength prediction by ANN formulation approach for FRP confined rectangular concrete columns. Journal of Rehabilitation in Civil Engineering, 2019, Vol. 7, No. 3, pp. 182-203.

[36] Sharifi Y., Moghbeli A., Hosseinpour M. and Sharifi H. Neural networks for lateral torsional buckling strength assessment of cellular steel I-beams. Advances in Structural Engineering, 2019, Vol. 22, No. 9, pp. 2192-2202.

[37] Sharifi Y., Moghbeli A., Hosseinpour M. and Sharifi H. Study of Neural Network Models for the Ultimate Capacities of Cellular Steel Beams. Iran J Sci Technol Trans Civ Eng, (2020) 44:579–589.

[38] Sharifi Y., Hosseinpour M., Moghbeli A., and Sharifi H. Lateral Torsional Buckling Capacity Assessment of Castellated Steel Beams Using Artificial Neural Networks. Int J Steel Struct, 2019, Vol. 19, 1408–1420.

[39] Sharifi Y., Mohammadi N., and Moghbeli A. Shear capacity assessment of reinforced concrete deep beams using artificial neural network. Journal of Concrete Structures and Materials, 2018, Vol. 3, No. 5, pp. 30-43.

[40] Tohidi, S. and Sharifi, Y. (2015). Neural networks for inelastic distortional buckling capacity assessment of steel I-beams. Thin-Walled Structures, Vol. 94, No. 9, pp. 359-371.

[41] Tohidi, S. and Sharifi, Y. (2014). Inelastic lateral-torsional buckling capacity of corroded web opening steel beams using artificial neural networks. The IES Journal Part A: Civil & Structural Engineering, Vol. 8, No. 1, pp. 24-40.

[42] Sharifi, Y. and Tohidi, S. (2014). Lateral-torsional buckling capacity assessment of web opening steel girders by artificial neural networks–elastic investigation. Frontiers of Structural and Civil Engineering, Vol. 8, No. 2, pp. 167–177.

[43] Sharifi Y, Tohidi S. (2014). Ultimate Capacity Assessment of Web Plate Beams with Pitting Corrosion Subjected to Patch Loading by Artificial Neural Networks. Advanced Steel Construction, Vol. 10, No. 3, pp. 325-350.

[44] Tohidi, S. and Sharifi, Y. (2014). A new predictive model for restrained distortional buckling strength of half-through bridge girders using artificial neural network. KSCE Journal of Civil Engineering, Vol. 10, No. 3, pp. 325–350.

[45] Tohidi, S. and Sharifi, Y. (2014). Load-carrying capacity of locally corroded steel plate girder ends using artificial neural network. Thin-Walled Structures, Vol. 100, No. 1, pp. 48–61.

[46] Sharifi Y., Moghbeli A. Rahmatian M. and Moghbeli K. (2020). Shear Strength Assessment of Slender Reinforced Normal Concrete Beams using Artificial Neural Networks. Journal of Concrete Structures and Materials, Vol. 4, No. 8, pp. 173-190.

[47] Ghoddousi, P., Abbasi, A. M., Shahrokhinasab, E., Abedin, M. (2019). Prediction of Plastic Shrinkage Cracking of Self-Compacting Concrete. Advances in Civil Engineering, 2019.

[48] Cybenko, J. (1989), Approximations by super positions of a sigmoidal function, Math Control Signal Syst, 2, 303–14.

[49] Marquardt, D. (1963). An algorithm for least squares estimation of non-linear parameters. J Soc Ind Appl Math, Vol. 11, pp. 431–41.

[50] Hagan, M.T. Menhaj, M.B. (1994). Training feed forward networks with the Marquardt algorithm. IEEE Transactions on Neural Networks, Vol. 5, No. 6, pp. 861-867.

[51] Hristev R.M. (1998). The ANN book. GNU public license.

[52] Gandomi, A.H. Tabatabaei, S.M. Moradian, M.H. Radfar, A. Alavi, A.H. (2011). A New Prediction Model for the Load Capacity of Castellated Steel Beams. Journal of Constructional Steel Research, Vol. 67, pp. 1096-1105.

[53] Frank, IE. Todeschini, R. (1994). The data analysis handbook, Amsterdam: Elsevier.

[54] Gandomi, A.H. Mohammadzadeh, S. Pérez-Ordó˜nezc, J.L. Alavi A.H. (2014). Linear genetic programming for shear strength prediction of reinforced concrete beams without stirrups. Applied Soft Computing, Vol. 19, pp. 112–120.

[55] Smith, G.N. (1986). Probability and Statistics in Civil Engineering. Collins, London.

[56] Garson, G. D. (1991). Interpreting neural-network connection weights. AI Expert, Vol. 6, pp. 47–51.

[57] Gandomi, A.H. Alavi, A.H. Mousavi, M. Tabatabaei, S.M. (2011). A hybrid computational approach to derive new ground-motion prediction equations. Eng. Appl. Artif. Intell. Vol. 24, No. 4, pp. 717–732.

[58] Gandomi, A.H. Alavi, A.H. Sadegh Kazemi C. Gandomi, M. (2014). Formulation of shear strength of slender RC beams using gene expression programming, part I: Without shear reinforcement. Automation in Construction, Vol. 42, pp. 112–121.